4541-6003-R0000
10 May 1966

WAVE-PARTICLE INTERACTIONS IN THE SOLAR WIND

by

Frederick L. Scarf
Space Sciences Laboratory
TRW Systems

33389

Recent fluid dynamic calculations which include thermal conduction viscosity and the rotating magnetic field of the sun appear to explain the transition from a nearly static corona to the supersonic solar wind, however the conventional fluid equations are not valid when the mean free paths become large. In interplanetary space the solar wind represents a collisionless magnetized plasma, and various plasma instabilities become significant as wave-particle interactions replace particle-particle scattering. The extent to which the interplanetary plasma can be considered a fluid is assessed using recent experimental data, the possible forms of local acceleration processes are discussed, and some classes of experiments which might help to understand these phenomena are described.

Presented at the D.G.R.R. Symposium "Exploration of the Moon and Interplanetary Space," Munich, April 22, 1966. To be published in Raumfahrtforschung.

I. INTRODUCTION

About fifteen years ago, Biermann (1951) argued that interplanetary space must be filled at all times with corpuscles streaming from the sun. Several years later, Chapman (1957) demonstrated that the hot solar corona should extend throughout the inner solar system, and in 1958, Parker combined these ideas with the postulate that the solar wind and the extended solar corona are the same entity. Parker showed how a nonstationary corona would be accelerated to supersonic speeds, and all of these indirect arguments in favor of a continuous wind from the sun were finally confirmed by the electrostatic analyzer measurements on Mariner 2 (Snyder and Neugebauer, 1964; earlier experiments on the Luniks and Explorer 10 had detected solar plasma, but the measurements were not extensive enough to verify the hypothesis of continuous streaming).

In this paper we review some of the recent experimental and theoretical advances in the study of the solar wind. It is argued that analysis of the gross or macroscopic characteristics of the solar wind and its associated magnetic field will not suffice in the future, and that detailed study of microscopic particle distribution functions, plasma instabilities and wave-particle interactions will be required. Experiments to explore these phenomena place severe constraints on requirements for telemetry, plasma probe look angles, etc., and it can be anticipated that future experimenters will desire sophisticated interplanetary spacecraft capable of exploring the microscopic plasma processes.

II. THE FLUID MODELS OF THE WIND

Parker's original model (1958) of the non-static corona was based on several simplifying assumptions. The observed coronal scale heights, as determined from $n_e(r)$ measurements, indicated no appreciable decrease in coronal temperature out to (10-20) R_θ, although the uncertainties become significant beyond about 8 R_θ. Accordingly, it was assumed that the corona is isothermal with temperature T_o in a region between the base (r=a) and a radius r=b (8 R_θ < b < 20 R_θ), with an adiabatic temperature distribution ($T \sim n^{2/3}$) beyond r=b. Since T(r) was completely specified in terms of n(r), it sufficed to consider the continuity and momentum equations for the collisional coronal fluid; for steady radial flow these are

$$nur^2 = C = \text{constant} \tag{1}$$

$$nmu \frac{du}{dr} + \frac{GM_\theta mn}{r^2} + \frac{d}{dr} nkT = 0 \tag{2}$$

and in the isothermal region, Parker demonstrated that the solutions behave as shown in Fig. 1. The solar wind solution is accelerated through the sonic transition by the pressure gradient term, while the solar gravitational attraction acts as the "throat" of a nozzle making the transition possible. The slow or subsonic solutions cannot actually occur, because for these cases the rotating magnetic field of the sun produces large magnetic forces which invalidate Eq. (2) (Axford, Dessler and Gottlieb, 1963).

As an example of the consequences of this theory, consider $u(a) \simeq 30$ km/sec, $n(a) = 2\, n_e(a) \simeq 3 \times 10^8$ cm^{-3}, $T(a) \simeq 1.5 \times 10^6$ °K with $a = 1.06\, R_\odot$, $b = 13\, R_\odot$; then Eqs. (1), (2) predict $u(1\ \text{A.U.}) \simeq 550$ km/sec and $n_e(1\ \text{A.U.}) \simeq 50$ cm^{-3}. The velocity is in remarkably close agreement with experiment, although the observed density at one A.U. appears to be more nearly 5 cm^{-3}. However, considering the great simplifications and idealizations inherent in the use of Eqs. (1), (2), it must be acknowledged that the simple hydrodynamic model provides the basic explanation for the existence of the solar wind.

In the years since 1958, a great deal of theoretical effort has been devoted to analysis of the flow patterns and characteristics of the wind, using fluid models of increasing sophistication. Chapman's original static theory revealed that energy transport by thermal conduction must be of great importance throughout the extended corona, and the appropriate generalization for a streaming fluid involves the Navier-Stokes equations. For spherically symmetric flow, the energy-momentum equations are

$$mnu \frac{du}{dr} + \frac{d}{dr}(nkT) + \frac{nGM_\odot m}{r^2} = \frac{1}{r^3}\frac{d}{dr}(r^3\tau) \tag{3}$$

and

$$\frac{mu^2}{2} - \frac{GM_\odot m}{r} + \frac{5}{2}kT + \frac{r^2 q}{C} - \frac{r^2 \tau}{C} u = E \tag{4}$$

where

$$q = -\kappa \frac{dT}{dr} \tag{5}$$

$$\tau = \frac{4}{3} \mu \, r \frac{d}{dr} \left(\frac{u}{r} \right) , \tag{6}$$

$C = nur^2$. Here κ, μ represent the coefficients of conduction and viscosity, respectively, and for an ionized hydrogen gas we use (Spitzer, 1962)

$$\kappa \simeq 7.2 \times 10^{-7} \, T^{5/2} \text{ ergs/cm sec } °K \tag{7}$$

$$\mu \simeq 0.9 \times 10^{-16} \, T^{5/2} \text{ qm/cm sec.} \tag{8}$$

Thermal energy can be transported to great distances from the sun via the mechanisms indicated in Eq. (4), and therefore Parker carried out extensive analytical studies of the flow patterns associated with a smooth decrease in temperature. For instance, the momentum equation was solved for an effective equation of state, $p \sim n^{\alpha}$, with the polytrope index varying between unity (isothermal flow) and 5/3 (adiabatic flow). [Much of this work is summarized in "Interplanetary Dynamical Processes (Parker, 1963).] Analytical investigations of the full Navier-Stokes equations have also been carried out [see the comprehensive review, "Dynamical Theory of the Solar Wind" (Parker, 1965a)] but these calculations can generally be performed only for hypothetical coronal densities which differ greatly from those of the sun.

A definitive test of the hydrodynamic model of the actual solar wind requires numerical integration of the coupled set, Eqs. (3) - (8), and this has now been performed. The first numerical analysis was that of Noble and Scarf (1963) and (singular) solutions of the most general variety (finite conduction out to infinity) were obtained with neglect of viscosity. Scarf

and Noble (1965) also considered the full Navier-Stokes equations and described (singular) solutions with finite conduction and viscous stress as $r \to \infty$. Numerical studies of the special well-behaved solutions (purely convective energy at infinity) were obtained by Whang and Chang (1965, no viscosity) and Whang, Liu and Chang (1966, viscous). In all cases, no external heat source was inserted, a one-fluid model was considered, and the parameters were adjusted to fit the observed density and temperature near the coronal base.

One test of the success of such a computation as an "explanation" for the solar wind involves comparison of the theoretical $n_e(r)$-curve (derived from $nur^2 = C$ and Eqs. (3) - (8)) with observation. The results are shown in Fig. (2) (taken from Whang, Liu and Chang). It can be seen that in the entire lower corona ($r < 10\text{-}20\ R_\odot$), with the possible exception of the base region below (2-2.5) $R_\odot$, the predicted densities are in very good agreement with observation. Since the transition to supersonic flow occurs near 7 $R_\odot$ for these solutions, it appears that the ultimate source of energy for the solar wind is simply transport of thermal energy from the base region via conduction (viscosity is completely negligible within 10 $R_\odot$ and no external energy source has been used).

For the solutions shown in Fig. (2), the predicted speeds near the earth are on the order of (200-300) km/sec, the densities are on the order of (1-10) cm^{-3}, and the anticipated temperatures are on the order of (1-2) x 10^5 °K. These numbers are all in fair agreement with the results of early measurements of the solar wind near 1 A.U., and one might therefore conclude that the fluid model provides an adequate description of the corona and the wind, all the way to the earth. However, more detailed inspection of these

results reveals significant internal inconsistencies and, indeed, it turns out that the predictions of Eqs. (3) - (8) become invalid long before the earth is reached.

III. BREAKDOWN OF THE MACROSCOPIC EQUATIONS

The continum fluid equations are only meaningful when the plasma is in strict (collisional) thermal equilibrium, and Sturrock and Hartle (1966) recently observed that even close to the sun, particle-particle collisions do not provide a mechanism for maintaining thermal equilibrium between electrons and protons. Using the electron-proton collision frequency

$$\nu_E = 8.5 \times 10^{-2}\ nT^{-3/2} \tag{9}$$

and <u>separate</u> coefficients of thermal conduction

$$\kappa_p \simeq 1.4 \times 10^{-8}\ T_p^{5/2},\ \kappa_e \simeq 6 \times 10^{-7}\ T_e^{5/2} \tag{10}$$

they considered a non-viscous two-fluid model. The energy balance equation for the protons was taken to be

$$\frac{3}{2}\, n\, \frac{dkT_p}{dr} - kT_p\, \frac{dn}{dr} = \frac{n}{C}\, \frac{d}{dr}\left(r^2 \kappa_p\, \frac{dT_p}{dr}\right) + \frac{3}{2}\, \frac{n}{u}\, \nu_E\, k\, \frac{\left[T_e - T_p\right]}{T_p} \tag{11}$$

and a similar expression described the energy balance for the electron fluid. Approximate numerical solutions to these coupled equations were obtained assuming equal temperatures near the base, with separate slowly varying polytrope indices for the electrons and protons. The best fit solutions near the base region were associated with the following parameters near 1 A.U.: $u \simeq$ 280 km/sec, $n \simeq 10\ cm^{-3}$, $T_p \simeq (3\text{-}4) \times 10^3$ °K, $T_e \simeq 6 \times 10^5$ °K.

The calculated velocity and density profiles are, as before, in fair agreement with observations, and to date no accurate measurements of the interplanetary electron temperature are available for comparison. However, the observed proton temperatures in the solar wind are generally considerably higher than these computed values, frequently ranging up to 10^6 °K, and rarely falling much below 3×10^4 °K (Neugebauer and Snyder, 1966; Strong, et al, 1966). This discrepancy strongly suggests that the fluid model should be abandoned much closer to the sun than 1 A.U.

A related conclusion can be derived by inspection of the one-fluid Navier-Stokes equations. As noted above, the general solutions to the coupled equations are singular in that they can be rewritten in the forms $dT/dr = G/\kappa(T)$, $du/dr = F/\mu(T)$ where G and F are functions of u, n, r, T, etc. This shows explicitly that not all solutions with finite κ, μ can be obtained by perturbation techniques starting with $\kappa = \mu = 0$. Indeed, in the supersonic region formal solutions exist for which $T \to 0$, $u \to \infty$ at some finite radius, and thus meaningless flow patterns can be obtained. However, these apparently meaningless predictions are quite significant physically; they can be used to illustrate the fact that the Navier-Stokes equations are invalid well before the singularity is reached.

The Navier-Stokes equations are derived from the Boltzmann equations by the Chapman-Enskog technique and they are valid wherever the Knudsen number (ratio of mean free path ℓ, to scale length L) is small compared to unity. The transport coefficients are evaluated by expanding all

functions in powers of (ℓ/L), and the conventional definitions (Eqs. (5), (6)) are then correct to first order in ℓ/L. For instance, the successive approximations to the viscous stress are

$$\tau_{ij}^{(0)} = 0,$$

$$\tau_{ij}^{(1)} = \mu\, \epsilon_{ij} \tag{12}$$

$$\tau_{ij}^{(2)} = \mu\, \epsilon_{ij} + \frac{\mu^2}{nkT}\, \epsilon_{ij}\, \vec{\nabla}\cdot\vec{u} + \ldots.$$

etc., where

$$\epsilon_{ij} = \frac{\partial u_i}{\partial X_j} + \frac{\partial u_j}{\partial X_i} - \frac{2}{3}\, \delta_{ij}\, \vec{\nabla}\cdot\vec{u} \tag{13}$$

(Schaaf and Chambrè, 1961) and

$$\mu \simeq n\, m^{1/2}\, (kT)^{1/2}\, \ell \tag{14}$$

(Eqs. (8), (9). This yields Eq. (6) if the second term in $\tau_{ij}^{(2)}$ can be neglected with respect to the first term. Thus, Eq. (6) is correct only if

$$\frac{\ell}{L_u} \left(\frac{mu^2}{kT}\right)^{1/2} << 1,\ L_u \left|du/dr\right| \simeq u \tag{15}$$

and the appropriate scale length turns out to be the one associated with the streaming velocity. (This is not a statement of general validity. The complete

expression for $\tau_{ij}^{(2)}$ contains temperature gradients as well. The Navier-Stokes equations become questionable whenever one of these terms is significantly large. In the solar wind case, the velocity gradients are steep beyond the sonic crossover while the thermal gradients remain moderate.) By inspection of the numerical solution, Scarf and Noble (1964) pointed out that the above inequality is not satisfied beyond $r = 20\ R_\odot$.

In the language of aerodynamics, we pass from the continuum region to the "slip flow" region when the appropriate Knudsen number approaches unity. For a neutral gas, the slip flow regime is bounded by the region of continuum flow ($\ell \ll L$) and free molecular flow ($\ell \gg L$). Actually, because the solar wind is a magnetized plasma, there is no region in which free flow occurs in the classical gasdynamics sense. Nevertheless, we can define three regions. For $(\mu\vec{\nabla}\cdot\vec{u}/nkT) \ll 1$, the full Navier-Stokes equations are valid. For $\mu(\vec{\nabla}\cdot\vec{u})/nkT \sim 1$, but $\ell\left|dT/dr\right| \ll T$, the Navier-Stokes equations are not valid, but there are enough collisions to maintain a statistical distribution function with a well-defined temperature. For $\ell\left|dT/dr\right| \geq T$, ordinary two-body collisions are unimportant and the characteristics of the particle distribution functions are determined by other phenomena.

In ordinary gasdynamics no rigorous formulation of the equations of motion is available for slip flow. Various complex systems of equations (the Burnett equations, the Thirteen Moment equations) have been proposed to replace the Navier-Stokes equations for moderate Knudsen numbers, but these replacements introduce severe difficulties, and considerable doubt exists about their physical validity. (Schaaf and Chambré, 1961, pp. 31-34.)

It seems likely that no moment equations will really be of use here, so that the flow patterns have to be obtained by solving the Boltzmann equation itself. However, it appears that the Navier-Stokes equations, with some modifications, provide a better description of the gas in the slip flow regime than the higher order systems.

This discussion indicates that at present no rigorous treatment of the solar wind flow is possible beyond (15-20) R_θ. In order to obtain some bound to the range of flow patterns, Scarf and Noble (1964) arbitrarily assumed that the Navier-Stokes equations are strictly valid up to 17 R_θ, with adiabatic continuum flow beyond 17 R_θ. The results for a quiet solar wind are shown in Table I. Although these numbers obviously are subject to considerable revision as more realistic treatments of the region beyond (15-20) R_θ are considered, the entries can be used to evaluate roughly the range of importance of two-body collisions. We find $\ell(T,n)\ dT/dr \simeq T$ for $r \simeq 75\ R_\theta$, and two-body collisions cannot serve to maintain the Boltzmann distribution function beyond this radius. Thus, the close agreement between the distributions frequently observed at the earth and a Boltzmann distribution indicates that some mechanism other than two-particle scattering binds the solar wind into a fluid and maintains the statistical spectrum beyond (70-100) R_θ.

Table 1. Model Quiet Solar Wind
($A = 100$, $T_0 = 1.5 \times 10^6$ °K, $m = 0.62\ m_{prot.}$)

$r/R_\odot$	u (km/sec)	N_e (cm^{-3})	T (°K)	Remarks
<2	--	--	--	"heating region"
2	18.4	2.03×10^6	1.47×10^6	
4.5	72.4	1.02×10^5	1.03×10^6	
6.8	105	3.09×10^4	8.89×10^5	
	(sonic transition near $r/R_\odot = 7$)			Uninhibited conduction and viscosity
7.2	110	2.62×10^4	8.73×10^5	
10	146	1.02×10^4	7.92×10^5	
12.6	190	4.95×10^3	7.55×10^5	
15	246	2.70×10^3	7.35×10^5	
20	267	1.40×10^3	4.8×10^5	
40	286	3.27×10^2	1.8×10^5	Adiabatic continuum flow
50	287	2.09×10^2	1.35×10^5	
80	290	81.5		
120	290	35.8		Collisionless flow dominated by scattering from magnetic and electric fluctuations
200	290	12.9		
215	290	11.2		

IV. WAVE-PARTICLE INTERACTIONS

The available evidence strongly suggests that some mechanism provides a means for maintaining a kind of statistical equilibrium in the wind well into the collisionless region. That is, the distributions are generally fairly "Maxwellian" near the earth, although the mean free path is huge [ℓ(1 AU) $\simeq$ 1 A.U.]. This possibility was anticipated by Parker (1958) in his original paper. It was suggested that various plasma instabilities would develop and that single particles would then interact strongly with organized groups of particles, or waves. If these wave-particle interactions involved turbulent scattering, they could then serve to maintain a fluid-like behavior well into the collisionless region. More recently, the concept of interplanetary acceleration by a collisionless wave-particle interaction has been examined (Parker, 1965b). In laboratory beam-plasma experiments, X-rays associated with locally produced superthermal electrons are readily detected [see references in Parker's article (1965b)]. This process could provide an alternate explanation for the slow decrease of the isotropic soft component following a great flare. Instead of attributing all of this to scattering of solar cosmic rays by a disordered magnetic shell beyond the earth (Meyers, Parker and Simpson, 1956). we might consider the possibility that the storm produces waves which accelerate particles as the oscillations damp away.

The collisionless magnetized interplanetary plasma admits a great variety of wave motions. For $\vec{k}$ nearly parallel to $\vec{B}$, a hydrogen plasma with B $\simeq$ 5 gamma, n $\simeq$ 5/cm^3 has modes listed in Table II. The ambient wave amplitudes are generally determined by the net balance between Cerenkov radiation and Landau or cyclotron damping, or, in other words, by the details

Table 2. Interplanetary Wave Modes

For k parallel to B, N = $5/cm^3$, B = 5 gamma, and no alpha particles, the modes are

Classification	Frequency Range	Comments	
Alfven Waves	$0 < f < f_c^+ \simeq 0.076/cm^3$	Ion Resonant	These are the Alfven and fast modes for $f \ll f_c^+$
Magnetosonic Waves	$0 < f < f_c^- \simeq 140$ c/s	Whistler Mode	
Electron Plasma Oscillations	$F \simeq f_p^- \simeq 20$ kc/s	Electrostatic	Non-propagating in a cold plasma
Lower Hybrid Resonance	$f \sim (f_c^+ f_c^-)^{1/2} = 10.6$ c/s	Electrostatic	
Upper Hybrid Resonance	$f \sim (f_p^{-2}+f_c^{-2})^{1/2} \simeq 20$ kc/s	Electrostatic	
Ion Waves	$0 < f < f_p^+ \simeq 465$ c/s	Electrostatic	These waves are not present in a cold plasma
Cyclotron Harmonics	nf_c^+, $n > 1$	Quasi-Electrostatic	

The wave amplitudes are determined by the net balance between Cerenkov radiation and Landau or cyclotron absorption.

Large amplitudes are associated with non-Maxwellian tails, superthermal particles, unequal ion-electron temperatures, electron-proton drifts, or velocity space anisotropies

of the particle distribution functions. For the electrostatic modes, the absolute minimum background levels are determined by a form of equipartition between mechanical and electrical energy. In particular, for the electron plasma oscillation branch, Rostoker (1961) has shown that an equilibrium plasma has

$$\frac{E^2}{8\pi} > \frac{1}{(2\pi)^3} \int \frac{kT_e}{2} \frac{K_D^2}{k_o^2 + K_D^2} \, d^3k_o \tag{16}$$

where $K_D^{-1} = L_D$ is the Debye length; $T \simeq 10^5$ °K, gives $L_D \simeq 10$ meters and the minimum electron plasma oscillation field amplitude is then on the order of 5 microvolts/meter for those oscillations with $\lambda \geq L_D$. More generally, this background amplitude is strongly dependent on the relative fraction of particles having speeds equal to or greater than the wave speed, since these are the particles which give up energy to the wave. Thus, Eq. (16) applies if the distribution is Maxwellian, but if a superthermal high energy tail is present, the background field can be orders of magnitude higher than the value quoted (Tidman, 1965).

The thermal background levels for the other wave modes are obtained by similar methods. Crudely speaking, the equilibrium background level for a given mode is on the order of

$$\frac{(E_{min})^2}{4\pi} \approx \frac{kT}{(L_{min})^3} \, . \tag{17}$$

For electrostatic (longitudinal) modes, $L_{min} \simeq$ the Debye length and for electromagnetic (transverse) modes, $L_{min} \gtrsim (kT/m)^{1/2}/f_c$ where $f_c = eB/2\pi mc$.

Estimates of the equilibrium background levels are only of limited importance because, as indicated above, a variety of deviations from equilibrium lower the damping and increase the Cerenkov radiation, yielding field enhancements. These include the presence of non-Maxwellian tails, unequal electron-proton temperatures, currents, superthermal particles and velocity space anisotropies. Indeed, these phenomena may be sufficiently important to overwhelm the damping so that an instability sets in and waves grow spontaneously.

Parker (1957, 1958) first proposed that in the solar wind particle scattering from waves associated with plasma instabilities could replace particle-particle scattering and maintain the fluid-like behavior in the collisionless region. Parker considered the long wavelength (mhd) limit and examined the consequences of magnetically aligned thermal anisotropies, such as a difference in parallel and perpendicular temperatures associated with a rest frame distribution function of the form

$$f(\vec{v}) = n\left(\frac{m}{2\pi}\right)^{3/2} \frac{1}{kT_\perp (kT_{||})^{1/2}} \exp\left[-\frac{m}{2k}\left(\frac{v_\perp^2}{T_\perp} + \frac{v_{||}^2}{T_{||}}\right)\right]. \qquad (18)$$

It was shown that transverse (magnetosonic) waves would grow spontaneously if

$$nk(T_{\|}-T_{\perp}) > \frac{B^2}{4\pi} \quad . \tag{19}$$

This "firehose" instability occurs because the centrifugal acceleration around the curving (i.e. perturbed) magnetic field gives rise to a current which enhances the irregularity. In the other extreme the "mirror" instability sets in and Alfvèn waves grow. That is, the system is unstable with respect to interchange if

$$\frac{(nkT_{\perp})^2}{nkT_{\|}} > \frac{B^2}{8\pi} \tag{20}$$

and the plasma flows into those parts of the wave where the field is weak, increasing $P_{\perp}$ and forcing the field lines farther apart. This further weakens the field and the waves grow.

These restrictions lead to a relatively small range of values for $T_{\|}$, $T_{\perp}$ which are stable against mhd perturbations and the appropriate limits are shown in Fig. (3). Even so, the mhd calculations which are only valid for low wave frequencies ($f << f_c^+, f_c^-$) are unduly optimistic. Indeed, if the stability conditions for finite frequencies are examined, it can be ascertained that <u>any</u> thermal anisotropy leads to growing electromagnetic waves. For instance, it has been shown (Stix, 1962; Noerdlinger, 1964; Kennel and

Petschek, 1966) using the Boltzmann equation with f given by Eq. (18) that magnetosonic waves with angular frequency ω decay as exp $(-\gamma t)$, with a damping rate given by

$$\gamma = \frac{\pi^2}{k} \frac{(\Omega_c^+ + \omega)^3}{(1+\omega/2\Omega_c^+)} \left[\frac{T_\perp - T_{||}}{T_{||}} + \frac{\omega}{\omega+\Omega_c^+} \right] \int_o^\infty v_\perp dv_\perp f(v_\perp, v_{||}=V_R) \qquad (21)$$

where $\Omega_c^+ = 2\pi f_c^+$, and $V_R = (B^2/4\pi nm)^{1/2} (\Omega_c^+/\omega)^{1/2} (1+\omega/\Omega_c^+)^{3/2}$. If $T_{||} > T_\perp$, γ can change sign and waves with $\omega/\Omega_c^+ + 1 < T_{||}/T_\perp$ will grow spontaneously. This generalized form of the firehose instability arises because protons with parallel velocities greater than or equal to V_R can feed energy into an (electron resonant) whistler mode wave traveling in the opposite direction. If $T_{||} > T_\perp$, there is a net excess of protons going fast enough so that they radiate energy, and growth results.

The analog of the mirror instability occurs for any finite $T_\perp > T_{||}$ (Kennel and Petschek, 1966). If $T_\perp^+ > T_{||}^+$ ion cyclotron (Alfvén) waves grow and if $T_\perp^- > T_{||}^-$, magnetosonic (whistler) modes grow, near the ion and electron cyclotron frequencies respectively. If $T_\perp > T_{||}$ electrostatic instabilities also arise. For $f_c^+ >> f_p^+$ the Harris instability (1961) is relevant and the ion cyclotron harmonics grow, but if $f_p^+ > f_c^+$, this is transformed to the Rosenbluth-Post instability (1965) and ion acoustic waves with $f \simeq f_p^+$ appear.

All of these velocity space plasma instabilities are meaningful when the properties of some uniform element of the solar wind are considered. Additional possibilities are present in interaction regions associated with changing solar wind parameters. When fast solar wind streams overtake slow

ones, collisonless instabilities of the classical two-stream variety can arise. As one example, consider a hypothetical situation with $\vec{B}$ parallel to $\vec{u}$; then in the rest frame of the slow wind, an incoming beam of protons with velocity $\Delta\vec{u}$ can feed energy into the electron whistler mode at frequencies near f_c^+ [see Eq. (21)] and these waves will have $\vec{k}$ vectors along $-(\Delta\vec{u})$. Since the group and phase velocities in the magnetosonic mode can be quite high at these low frequencies (Kennel and Petschek, 1966) it is conceivable that the waves may propagate upstream.

The electrostatic two-stream instability can also be relevant. If we consider a relative electron-proton drift speed, u_p, then the system will be unstable with respect to longitudinal plasma oscillations if u_p exceeds a critical speed $u_p^{(c)} = u_p^{(c)}(T_e, T_p)$. This threshold for instability is large if $T_e = T_p$, but it falls rapdily as T_e/T_p increases, as shown in Fig. (4) (taken from Bernstein, et al., 1964). The fastest growing waves are ion acoustic oscillations with $f \sim f_p^+$, $\lambda \sim L_D$ and if $T_p \simeq 10^5$ °K, $T_e/T_p \gg 1$, the critical drift speed is about 300 km/sec. Since the solar wind speed is on this order, any perturbation which peels the electrons from the protons can possibly trigger the ion acoustic wave instability.

A simple mechanism exists which can indeed produce both high electron temperatures and large electron-proton drift speeds when the solar wind direction and/or magnitude change. The solar wind flows through the inclined interplanetary magnetic field because in a inertial frame an interplanetary electric field is present with

$$\vec{E}_I = -\frac{\vec{u}\times\vec{B}}{c} \tag{22}$$

This field is very large and its fluctuations could produce currents which trigger ion wave instabilities. For u = 400 km/sec, B = 5 gamma, $E_I \simeq 2 \times 10^{-5}$ volts/cm. The criterion of large size involves comparison with the runaway field

$$E_R \simeq \frac{kT}{e} \left(\frac{m}{kT}\right)^{1/2} \nu_E \tag{23}$$

$$\simeq 2 \times 10^{-8} \frac{n}{T} \frac{\text{volts}}{\text{cm}}$$

where ν_E is given by Eq. (9). If a field applied parallel to $\vec{B}$ exceeds E_R, then the electron current increases as eEt/m (Spitzer) until the relative electron-proton speed exceeds the plasma oscillation speed. When this happens large amplitude plasma oscillations are radiated by the Cerenkov mechanism, the electrons are scattered, and this scattering produces warm electrons and a finite conductivity parallel to the magnetic field.

For $n = 10\ \text{cm}^{-3}$, $T \sim 2 \times 10^5$ °K, $E_R \sim 10^{-12}$ volts/cm and $E_I \simeq 2 \times 10^7\ E_R$, but the quiescent interplanetary electric field is normal to $\vec{B}_I$ and hence this does not produce runaway. However, it is clear that customary fluctuations in $\vec{B}$, $\vec{u}$ and cos $(\vec{B},\vec{u})$ can produce localized interface regions in which $(\vec{E}_I)_{||}$ exceeds E_R; we can expect very rapid growth of plasma oscillations at such interfaces.

The possible excitation of large amplitude oscillations in the interplanetary medium has several important consequences. First, many of these modes have phase and group velocities which exceed 300-400 km/sec (i.e., electron plasma oscillations and cyclotron harmonics, the electron whistler mode with 0.5 - 1.0 c/s < f << f_c^-, etc.) and if these waves are generated, they can propagate upstream as well as downstream. This degrades the analysis of any local "shock" jump relations and makes determination of the wave source position difficult. Second, the modes which are slow (ion acoustic waves, proton whistlers, electron whistlers with f < 0.5 - 1.0 c/s, etc.) can readily be made to grow to large amplitudes by the Cerenkov mechanism, and particles with various thermal velocities may "see" wave frequencies which are significantly Doppler shifted.

This last point is particularly significant because some particles will see wave frequencies Doppler shifted to local cyclotron frequencies and a very efficient cyclotron acceleration can then take place. For electrostatic waves the equations of motion are

$$m\ddot{\vec{r}} = e\vec{E}(\vec{r},t) + e\frac{\dot{\vec{r}}\times\vec{B}_o}{c} \tag{24}$$

$$\vec{E} = -\vec{\nabla}\phi,\ \phi = \phi_o \int F(\vec{k},t)\cos(\vec{k}\cdot\vec{r}-\omega t)\, d^3k \tag{25}$$

and a very likely source of electron acceleration ($f_c^- \simeq 140$ c/s) involves the ion acoustic branch (0 < f < 465 c/s) which actually overlaps the

gyrofrequency. Stix (1964) originally discussed such wave-particle interactions for laboratory experiments. Scarf, et al. (1965) and Fredricks et al. (1965) examined numerical solutions to equations (24), (25) and applied the results to the disturbed solar wind. They introduced a stochastic phase decoherence and showed how waves with $e\phi_o \simeq$ 500 ev, $E_{peak} \simeq$ 40 millivolts/meter, can produce 65 keV electrons in several milliseconds via the non-linear Doppler-shifted cyclotron resonance described by Eqs. (24), (25). A related investigation by Sturrock (1966) involved completely stochastic acceleration so that study of Eq. (24) alone was sufficient. It was shown that smaller electric fields acting over longer times could produce comparable final energies.

V. RECENT OBSERVATIONS

Until recently experiments on interplanetary spacecraft were designed to examine only the gross, quasi-static characteristics of the solar wind and the interplanetary field. Thus, the wide aperature ion traps on the Luniks, Explorers 10, 18, etc., obviously could not investigate details of the particle velocity distributions and the narrow aperature electrostatic analyzer on Mariner 2 was constrained to look only at the sun. Similarly, the analyzer on Explorer 18 yielded only very crude angular distributions (i.e., three sectors in spacecraft longitude, essentially no resolution in spacecraft latitude). The analyzers on OGO-1, VELA 2A, 2B, 3A, 3B had much better longitudinal resolution, but again the observed current represents an integral over the solar plasma direction of arrival with respect to the spacecraft latitude. The first experiment capable of obtaining the complete angular distribution of the solar wind is the NASA/Ames Research Center experiment on Pioneer 6.

The results of this experiment are remarkable. In general, it is found (Wolfe, et al., 1966) that the direction of arrival for solar protons depends strongly on the energy (or velocity) window under examination. The ARC group has shown that this phenomenon is a simple consequence of a rather extreme thermal anisotropy, as illustrated in Fig. (5). In the plasma rest frame $T_{\parallel} >> T_{\perp}$, where the subscripts refer to direction with respect to the skewed interplanetary magnetic field [Fig. (5a)]. In Fig. (5b) the same distribution is depicted, but the frame of reference is now one in which the mean solar wind velocity is $\vec{u}$. A natural consequence of $T_{\parallel} >> T_{\perp}$ is then a skewing of the vector distribution as illustrated.

Wolfe et al. (1966) found that the solar wind distribution in the rest frame is very nearly a bi-Maxwellian [Eq. (18)] with variable but large $K = T_{\parallel}/T_{\perp}$ ($K > 5$ is a common situation). The most likely origin of this anisotropy would appear to be conservation of the magnetic moment,

$$\mu = \frac{mv_{\perp}^2}{2B} \quad , \tag{26}$$

in the relatively quiet interplanetary magnetic field. That is, as the wind proceeds away from the sun the imbedded magnetic field declines with

$$B_r \sim \frac{1}{r^2} \quad , \quad B_\theta \sim \frac{1}{r} \tag{27}$$

and hence $m \langle v_{\perp}^2 \rangle / 2 \sim kT_{\perp}$ decreases accordingly. Since this decrease in $T_{\perp}$ must be conservative, $T_{\parallel}$ has to increase.

The observed K-values clearly place the solar wind in the fire-hose unstable region, as indicated in Fig. (3). However, the long wavelength mhd waves are not the fastest growing ones. Scarf, Wolfe and Silva (1966) inserted the observed distributions into Eq. (21) and showed that the fastest growing waves have frequencies near (1-2) f_c^+. In the neighborhood of 1 A.U., Eq. (21) indicates that whistler mode waves with $f \sim 0.07$ c/s - 0.16 c/s (in the plasma rest frame) should be unstable with significant growth rates. Thus, as a consequence of the anisotropic thermal distribution observed by Wolfe, et al. (see also Hundhausen, et al., 1966), it may be anticipated that significant "background" wave levels near f_c^+ are present, and one can also

expect that large amplitude waves at these frequencies are readily generated whenever the plasma is disturbed.

The wave data available are quite incomplete, but the measurements which have been made are very suggestive. Fig. (6) shows the composite interplanetary power spectral density of (dB/dt) based on Mariner 2 fluxgate measurements (Coleman, 1965) and search coil data from OGO-1 (Holzer, et al., 1966). It should be noted that Mariner 2 measured the power spectrum of B directly and this has been converted by multiplying by f^2 to obtain an equivalent search coil power spectrum. However, the rising power density as $f \to f_c^+$ is certainly significant since the day 278 curve is an order of magnitude higher than the day 272 results, and hence well above the fluxgate threshold sensitivity. The OGO-1 interplanetary signals, on the other hand, are quite weak and fairly near threshold (M. G. McLeod, private communication) so that further verification is desirable. However, additional evidence exists suggesting that large amplitude waves with periodicities on the order of 10 seconds are readily generated when the wind is disturbed. Indeed, the first spacecraft magnetometer to penetrate the transition region aboard Pioneer 1 detected short intense noise bursts with $f \sim 0.1$ c/s (Sonett, et al., 1959). Recent observations on the third launch VELA spacecraft (Greenstadt, et al., 1966) suggest that such oscillations can be triggered in what would appear to be interplanetary space, as shown in Fig. (7), although these measurements were taken close to the transition region and they may not be truly interplanetary.

In summary, the evidence suggests that the interplanetary medium is actually unstable with respect to the proton-driven electron-whistler mode interaction described by Eq. (21). Indeed, it is conceivable that some interplanetary "shock" interactions associated with fast streams overtaking slow ones may simply represent changes in the growth rates associated with an increase in the number of high energy protons which produce the Cerenkov radiation. A case in point involves the Mariner 2 storm of October 7, 1962 (Sonett, et al., 1964). The fast protons could have triggered large amplitude whistler mode waves which propagated upstream, accounting for the extensive magnetic disorder detected well after onset of the velocity change.

The above instability or the electrostatic ones can give rise to interplanetary stochastic particle acceleration. However, study of acceleration processes obviously requires analysis of electric fields, and to date no direct measurements have been performed in interplanetary space, so that any discussion must be rather speculative. On the other hand, the IMP-1 observations of superthermal electron spikes in and well beyond the earth's transition now point to an interplanetary acceleration process (Fan, et al., 1966), and greater than 40 kev electrons have been observed on Mariner 4 at great distances from the earth (Van Allen and Krimigis, 1965). Although impulsive emission from the sun, or Fermi acceleration are conceivable sources of high energy particles, wave-particle interactions are also plausible.

Some indirect evidence suggests that large amplitude plasma waves are present in interplanetary space. Meecham (1964) has shown that density oscillations disturb the forward scattering of RF waves having comparable wavelengths. If

$$h(R) = \frac{\delta n(\vec{r}+\vec{R})\,\delta n(\vec{r})}{\delta n(\vec{r})^2} \tag{28}$$

then the forward propagation equation for an RF wave with $k = 2\pi/\lambda$ is

$$\frac{c^2k^2}{\omega^2} \simeq 1 - \frac{\omega_p^2}{\omega^2} + \frac{\omega_p^4}{c^4k_o}\frac{\delta n^2}{n^2}\;\frac{1}{8\pi^2}\int k\,dk\,h(k)\;\ell n\left(\frac{k+2k_o}{k-2k_o}\right) \tag{29}$$

where $c^2k_o^2 = (\omega^2-\omega_p^2)$ and $h(k)$ is the Fourier transform of $h(R)$. Thus, if $h(k)$ has significant components near $2k_o$, the index is strongly modified and the RF wave may undergo scintillation. Coherent plasma oscillations can produce severe scintillation if the scale sizes are on the order of λ(R.F.)/2 (Scarf, 1966), and large amplitude low frequency interplanetary scintillation at 178 Mc/s (Hewish, et al., 1964), 195 Mc/s, 430 Mc/s and 611 Mc/s (Cohen, et al., 1966) has actually been observed.

If we assume that disturbed portions of interplanetary space are "similar" to the geomagnetic transition region, then the arguments in favor of stochastic acceleration associated with plasma instabilities become strengthened. Fig. (8) shows a typical transition region proton spectrum from OGO-1 on a day when the solar wind speed and temperature were 712 km/sec and 2×10^5 °K respectively (Wolfe, Silva and Myers, 1965). Simultaneous

observations on IMP-2 and VELA-2 revealed that the transition region plasma spectrum had the same peak energy, non-thermal tail, and general shape at widely separated observation points. This would indicate that the incident plasma has undergone a transition to a definite new state; Fredricks and Scarf (1965) proposed that the new state is simply one of marginal stability with respect to ion acoustic waves, as shown in Fig. (4), with $T_e/T_p >> 1$. The VELA observations (Coon, 1965) reveal that hot electrons ($E \sim 100$-500 eV) are present in the transition region, in addition to the localized spikes of energetic electrons ($E > 40$ keV), and since the proton distribution also has a significant non-thermal tail, it can be shown that the background plasma oscillation fields must be large throughout the transition region (Eviatar, 1966). However, a local acceleration process must have operated to produce both the hot electrons and the high energy protons, since neither group was present in the incident solar wind. One may anticipate that a similar efficient stochastic acceleration process is significant even far from the earth when the solar wind is disturbed.

VI. CONCLUSIONS

It is now apparent that the interplanetary medium can serve as a valuable plasma laboratory in which instabilities, non-linear processes and fundamental acceleration mechanisms may be explored without many of the degrading phenomena encountered in the laboratory, such as non-containment, wall effects, distortion of the plasma by the probes, etc. However, the necessary measurements are not easily obtained, and some effort must be devoted to design a spacecraft as a plasma laboratory. For instance, the skewed interplanetary proton distributions can not be analyzed without complete, high resolution angular and energy scans; indeed, a probe looking only at the sun would generally detect a peak at the wrong energy and a wide aperature instrument might obtain a false angular distribution, even on a spinning spacecraft. Furthermore, since the ARC Pioneer 6 experiment reveals that the solar wind flow direction has significant deviation from the mean (i.e., from radial flow in the ecliptic plane), it is clear that the aberration angle can fluctuate even when the speed remains constant and integrals over spacecraft latitude may give completely non-representative currents.

In order to operate a plasma laboratory in interplanetary space, it must be possible to detect all of the wave modes listed in Table 1. For the higher frequencies this is readily accomplished using E and B sensors with bandpass filters, but at the lowest frequencies various "aliasing" problems associated with multirate sampling, spin folding, etc., enter and great care must be exercised in designing the sampling and telemetry sequences.

[These same problems may contaminate attempts to measure the D.C. magnetic field in the presence of large amplitude magnetic fluctuations.] Finally, it is extremely difficult to distinguish between local electromagnetic or electrostatic disturbances and those which have propagated to the spacecraft. If a high telemetry rate is available it might be possible to measure dispersions (changing frequencies with time) which would indicate that the wave has propagated, but even so Doppler broadening can completely obscure this effect. It is most important that high sensitivity plasma probes be developed so that one can examine the actual fast local fluctuations in the densities and currents for electrons and protons separately.

Acknowledgments

I am grateful to J. Wolfe, R. Silva, P. Coleman, Jr., E. Greenstadt, and G. Inouye for stimulating discussions about their measurements and for permission to describe the results. This work was supported by the National Aeronautics and Space Administration under Contract NASW-1366.

FIGURE CAPTIONS

Figure 1. The steady state velocity profile for the Parker model of the solar corona. The high temperature in the base region is associated with pressure gradients which accelerate the corona to supersonic speeds.

Figure 2. Experimental observations of $N_e(r)$ in the solar corona, and calculated density profiles obtained by numerical integration of the Navier-Stokes equations [curve taken from Whang, Liu, and Chang (1966); see this article for experimental references].

Figure 3. Stable and unstable regions for long wavelength (mhd) Alfvèn and "fast" waves.

Figure 4. Stable and unstable regions for the ion acoustic wave drift instability.

Figure 5a. A field-aligned anisotropic distribution with $T_{\parallel} >> T_{\perp}$, as viewed in the plasma rest frame.

Figure 5b. The same distribution, as viewed in a frame for which the mean plasma velocity is $\vec{u}$.

Figure 6. Interplanetary power spectra. The Mariner 2 results (Coleman, 1965) have been converted to an equivalent search coil spectral density as discussed in the text.

Figure 7. Magnetic fluctuations with $T \simeq 13$ seconds recorded near the earth-sun line on VELA.

Figure 8. An OGO-A transition region spectrum showing rapid streaming and significant particle acceleration, as indicated by the appearance of a large non-Maxwellian high energy tail which was not present in the incident solar wind.

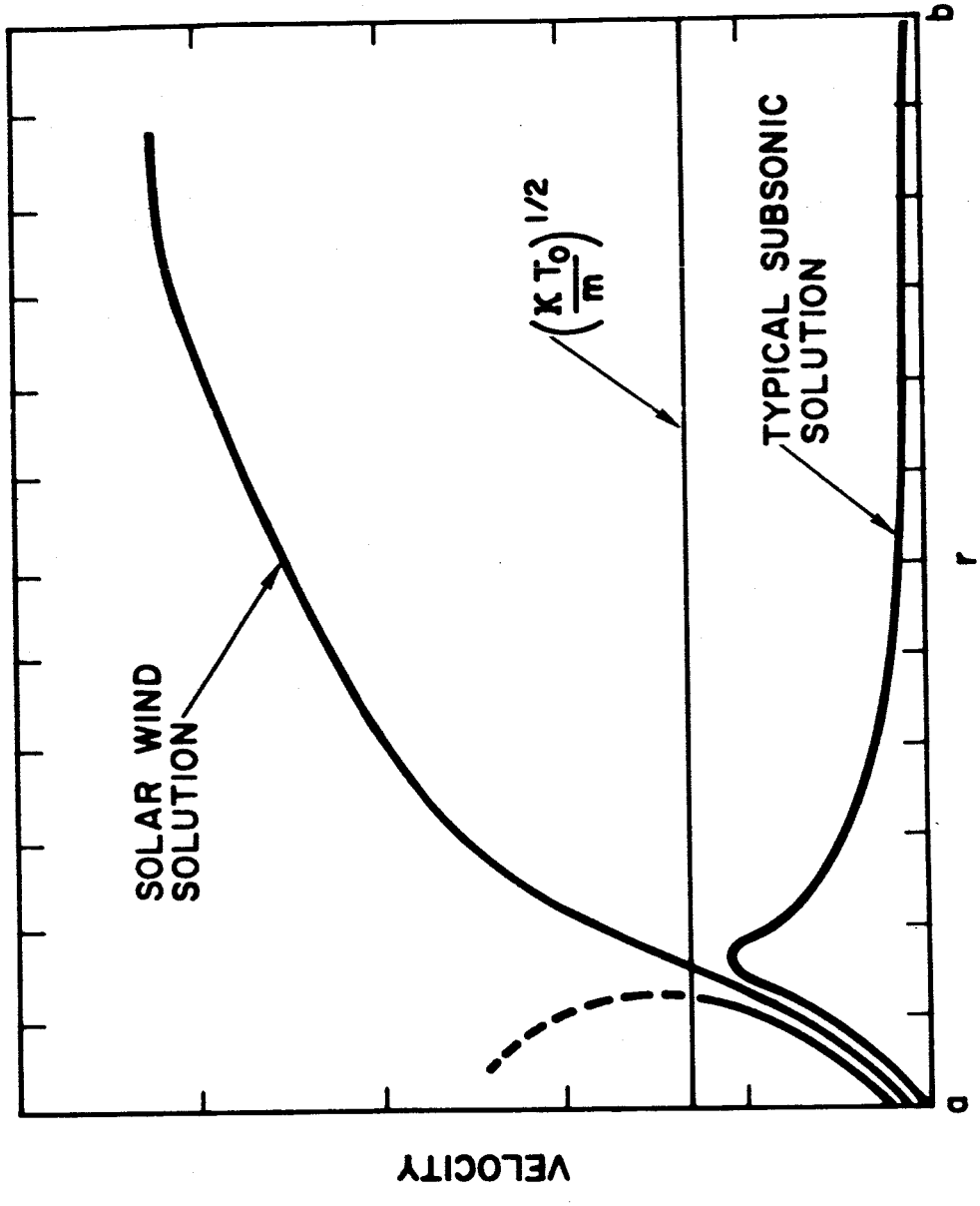
VELOCITY
r
a
b
SOLAR WIND SOLUTION
$\left(\frac{\kappa T_o}{m}\right)^{1/2}$
TYPICAL SUBSONIC SOLUTION

Figure 1.

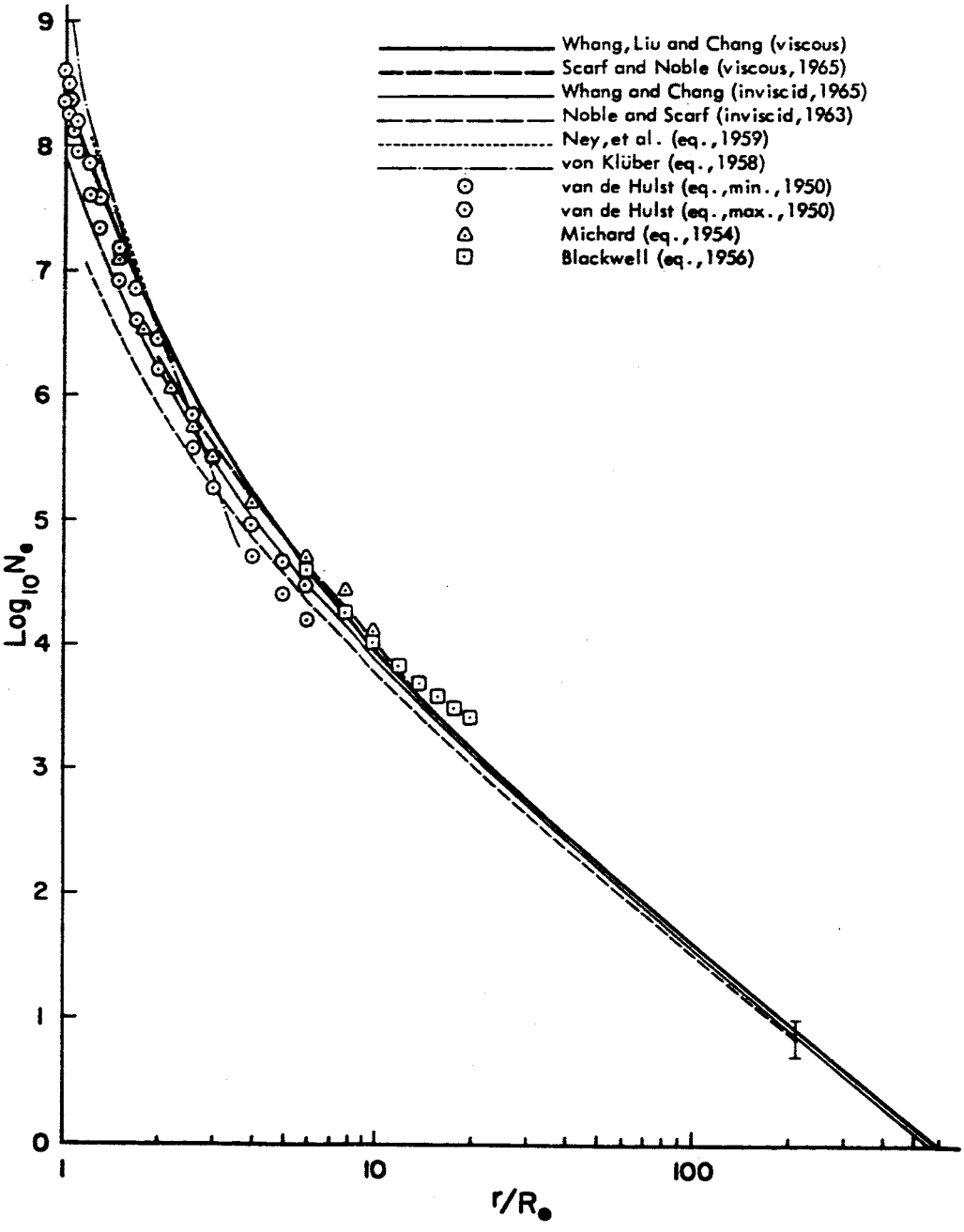
Whang, Liu and Chang (viscous)
Scarf and Noble (viscous, 1965)
Whang and Chang (inviscid, 1965)
Noble and Scarf (inviscid, 1963)
Ney, et al. (eq., 1959)
von Klüber (eq., 1958)
van de Hulst (eq., min., 1950)
van de Hulst (eq., max., 1950)
Michard (eq., 1954)
Blackwell (eq., 1956)
Log10N•
r/R•
0
1
2
3
4
5
6
7
8
9
1
10
100

Figure 2.

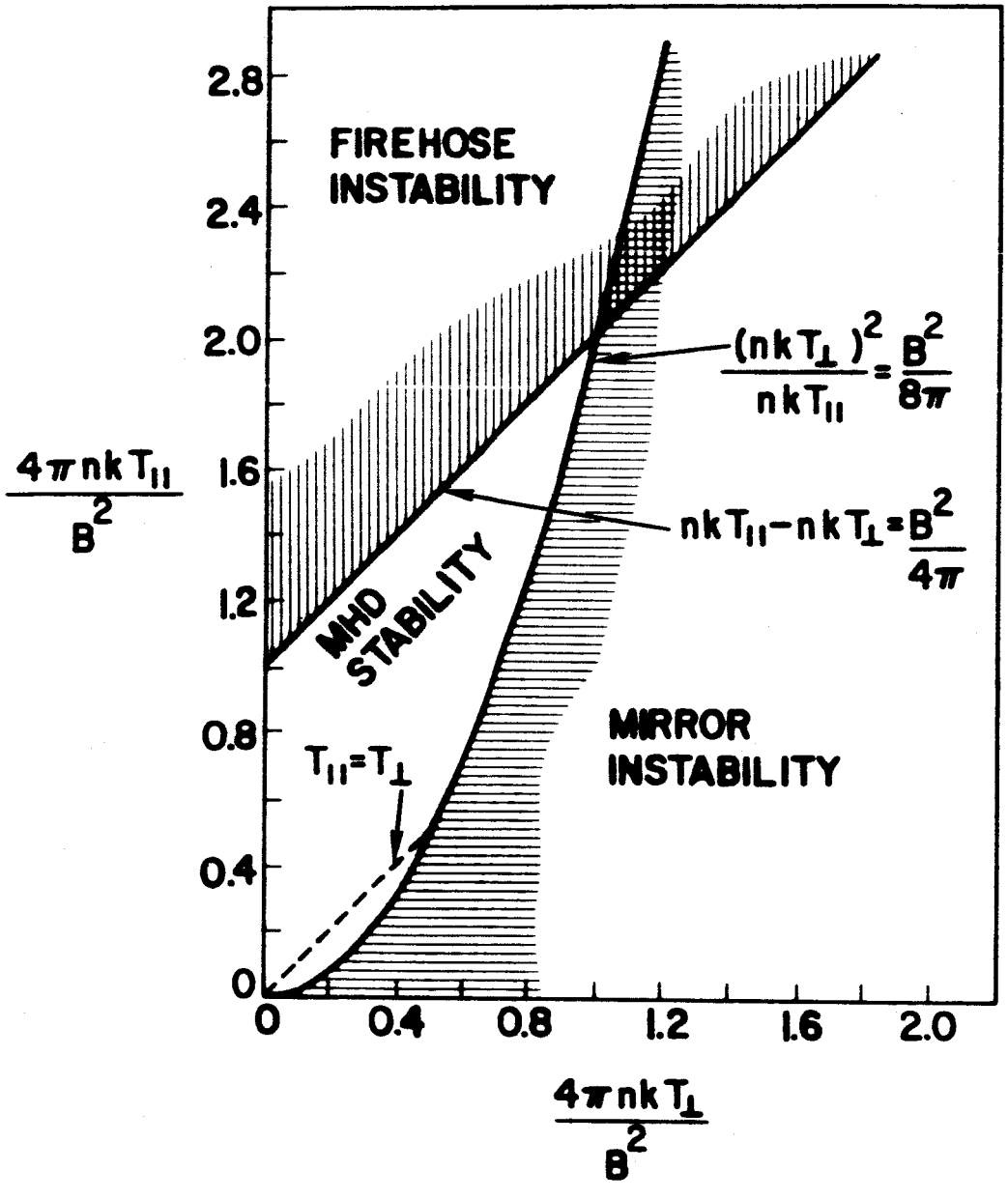
FIREHOSE
INSTABILITY
MHD
STABILITY
MIRROR
INSTABILITY
$T_{11}=T_\perp$
$\frac{(nkT_\perp)^2}{nkT_{11}}=\frac{B^2}{8\pi}$
$nkT_{11}-nkT_\perp=\frac{B^2}{4\pi}$
$\frac{4\pi nkT_{11}}{B^2}$
$\frac{4\pi nkT_\perp}{B^2}$
0
0.4
0.8
1.2
1.6
2.0
2.4
2.8

Figure 3.

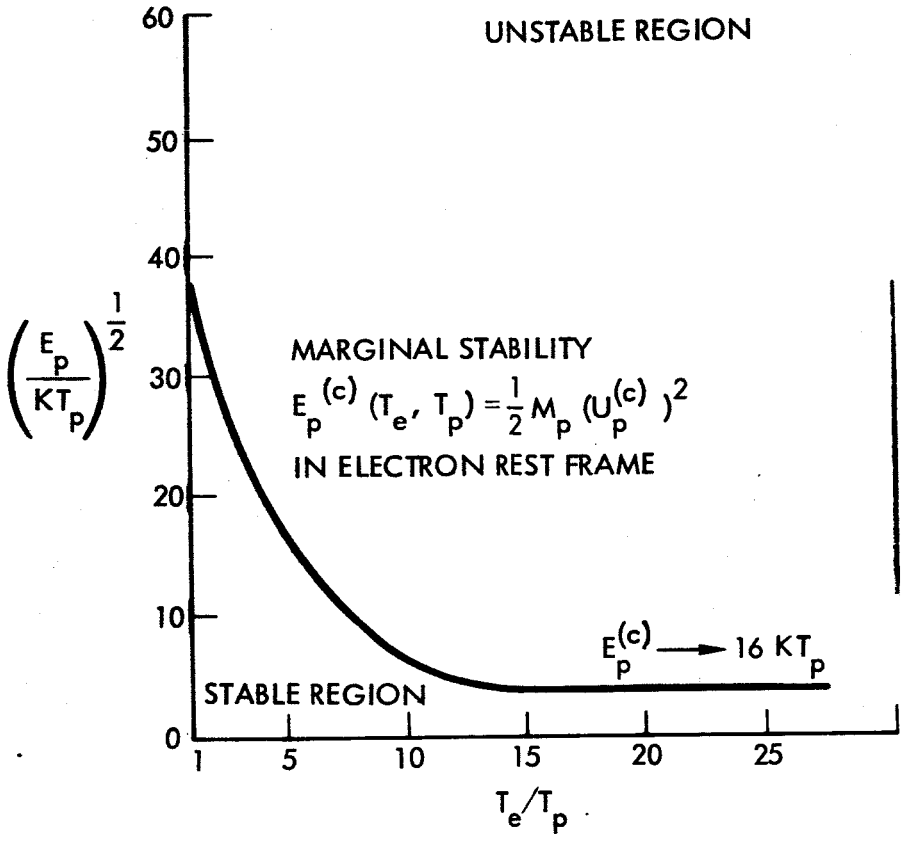
UNSTABLE REGION
60
50
40
30
20
10
0
$\left(\frac{E_p}{KT_p}\right)^{\frac{1}{2}}$
MARGINAL STABILITY
$E_p^{(c)}(T_e, T_p) = \frac{1}{2} M_p (U_p^{(c)})^2$
IN ELECTRON REST FRAME
$E_p^{(c)} \longrightarrow 16\ KT_p$
STABLE REGION
1
5
10
15
20
25
T_e/T_p

Figure 4.

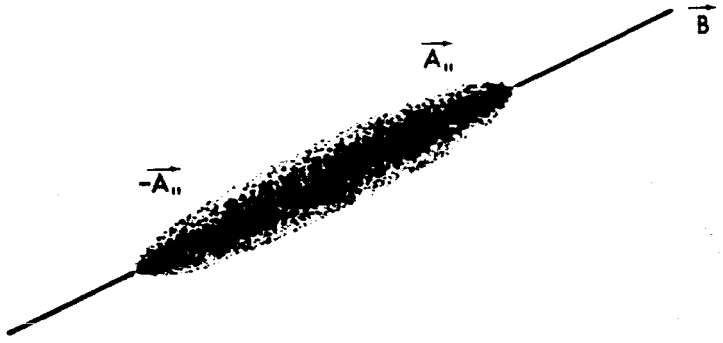
$\vec{B}$
$\vec{A}_{\parallel}$
$-\vec{A}_{\parallel}$

a)

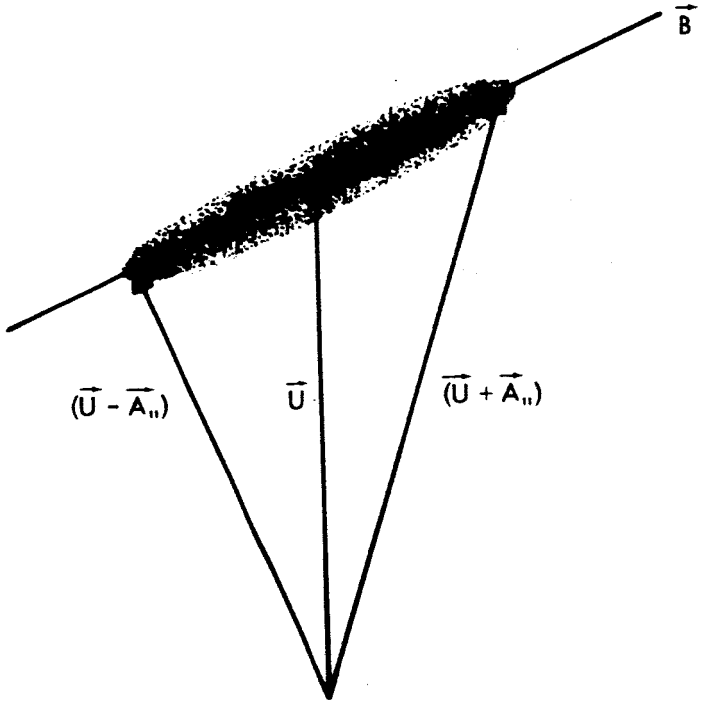
$\vec{B}$
$(\vec{U} - \vec{A}_{\parallel})$
$\vec{U}$
$(\vec{U} + \vec{A}_{\parallel})$

b)

Figure 5.

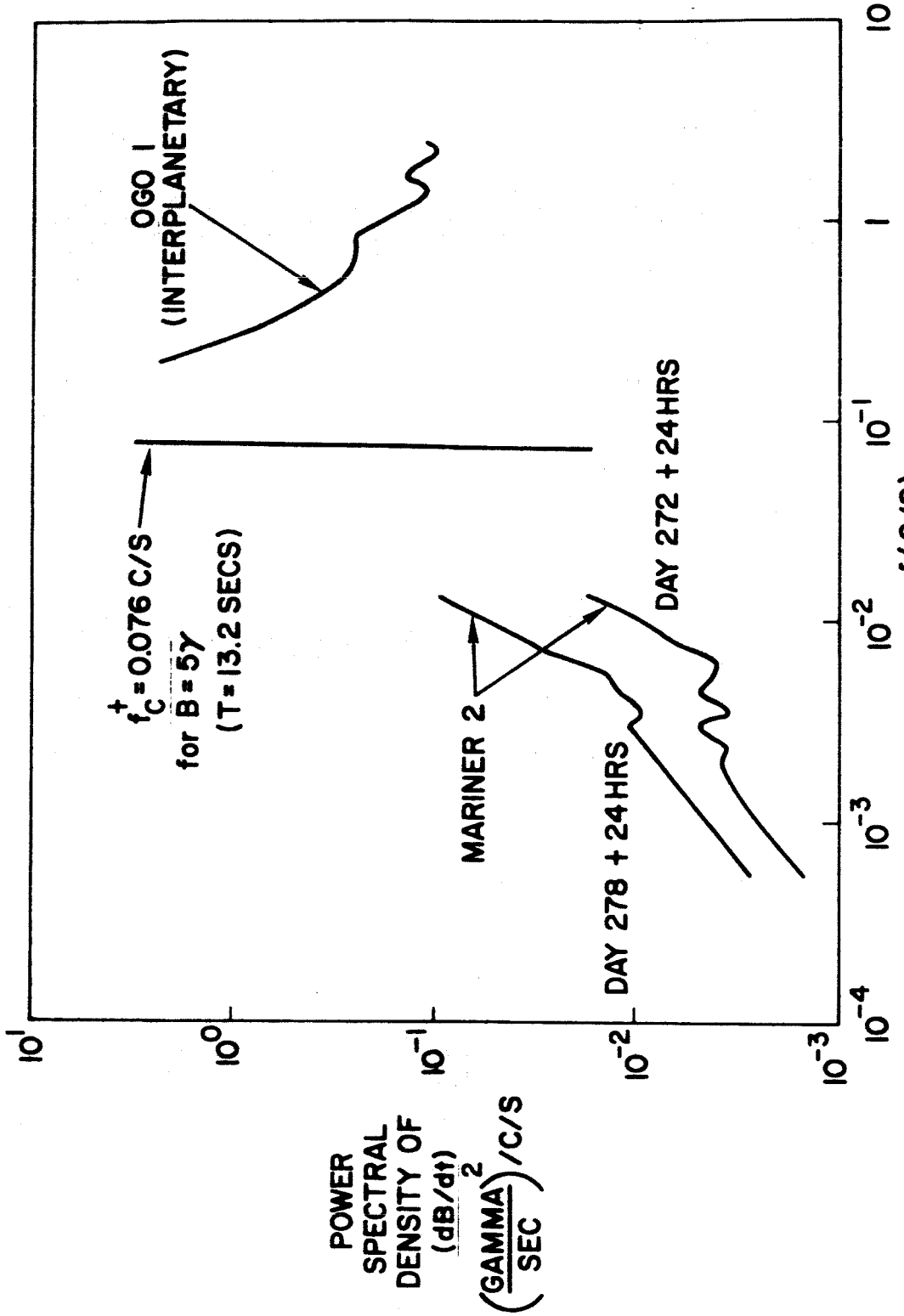
OGO 1
(INTERPLANETARY)
f_c^+ = 0.076 C/S
for $\bar{B}$ = 5γ
(T = 13.2 SECS)
MARINER 2
DAY 272 + 24 HRS
DAY 278 + 24 HRS
POWER SPECTRAL DENSITY OF (dB/dt)
$\left(\frac{\text{GAMMA}}{\text{SEC}}\right)^2$/C/S
f (C/S)
10^{1}
10^{0}
10^{-1}
10^{-2}
10^{-3}
10^{-4}
10
1
10^{-1}
10^{-2}
10^{-3}

Figure 6.

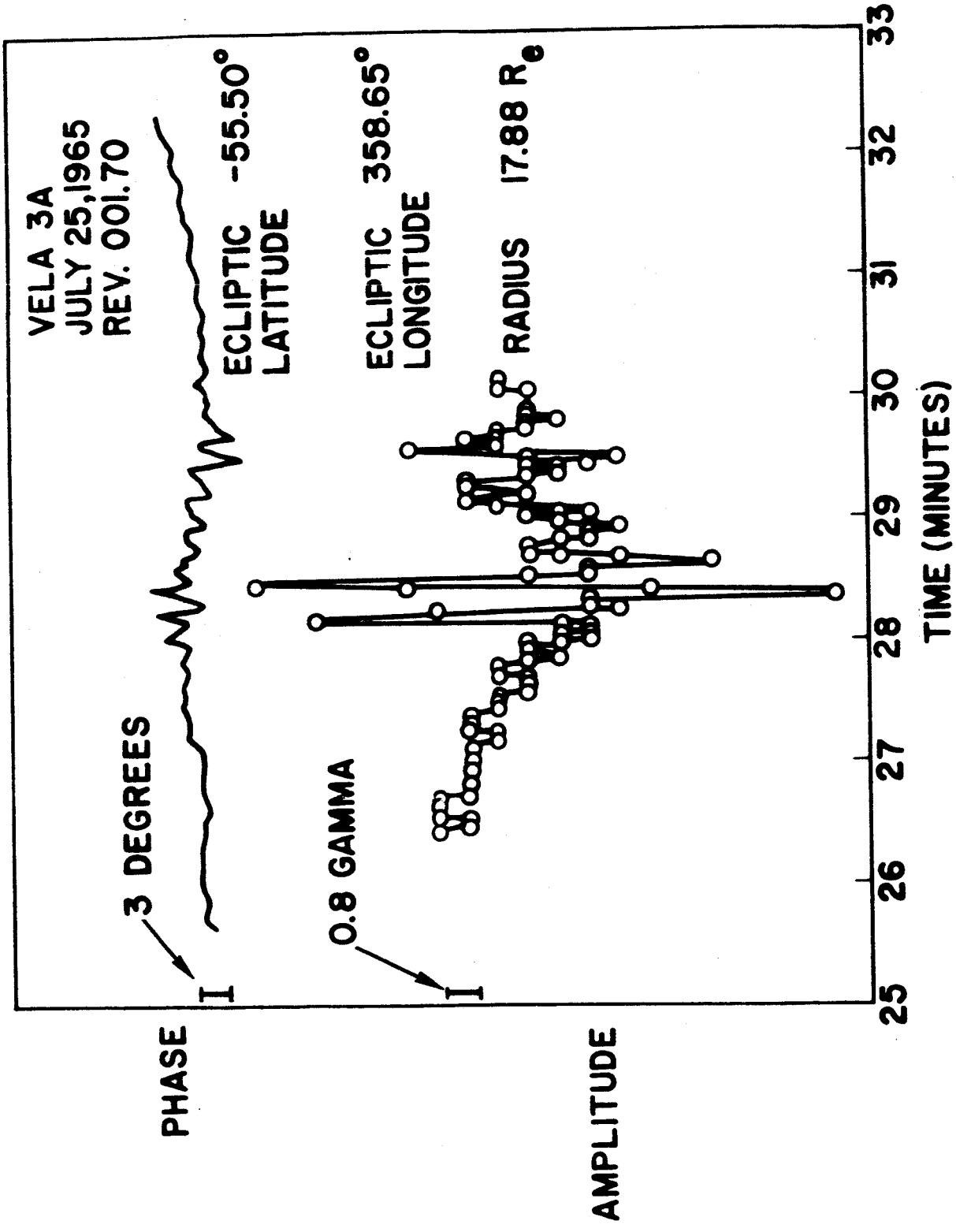
VELA 3A
JULY 25,1965
REV. 001.70
ECLIPTIC LATITUDE -55.50°
ECLIPTIC LONGITUDE 358.65°
RADIUS 17.88 R_e
3 DEGREES
0.8 GAMMA
PHASE
AMPLITUDE
25
26
27
28
29
30
31
32
33
TIME (MINUTES)

Figure 7.

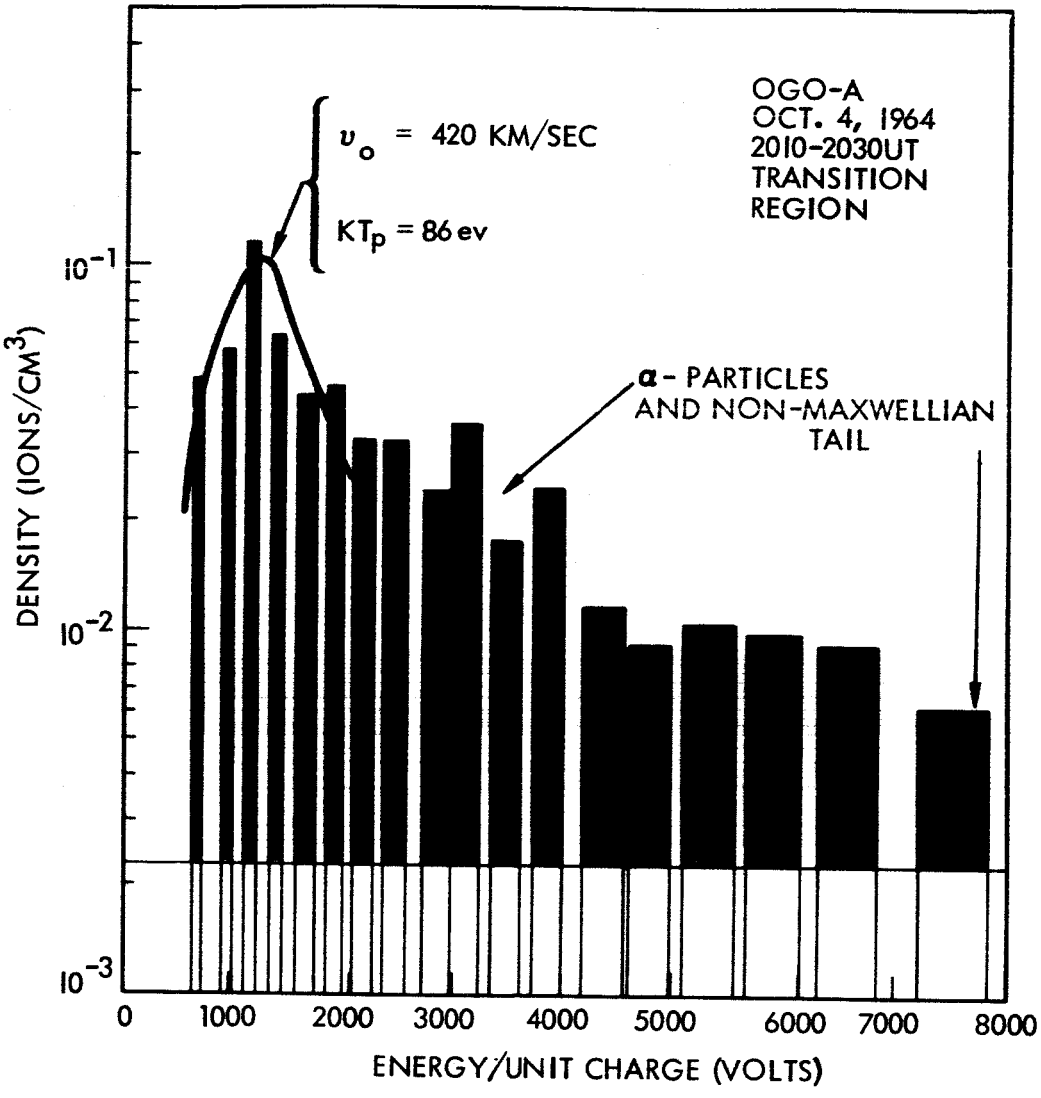
OGO-A
OCT. 4, 1964
2010-2030UT
TRANSITION
REGION
v_o = 420 KM/SEC
KT_p = 86 ev
α - PARTICLES
AND NON-MAXWELLIAN
TAIL
DENSITY (IONS/CM^3)
10^{-1}
10^{-2}
10^{-3}
0
1000
2000
3000
4000
5000
6000
7000
8000
ENERGY/UNIT CHARGE (VOLTS)

Figure 8.

REFERENCES

1. Axford, W. I., A. J. Dessler, and B. Gottlieb, Astrophys. J. 137, 1268, 1963.

2. Bernstein, W., R. W. Fredricks, and F. L. Scarf, J.G.R. 69, 1201, 1964.

3. Biermann, L., Z. Astrophys. 29, 274, 1948.

4. Chapman, S., Smith. Cont. Astrophys. 2, 1, 1957.

5. Cohen, M. H., H. E. Hardebeck, and L. E. Sharp, Spring U.R.S.I. Bull. 103, 1966.

6. Coleman, P., U.C.L.A. Ph.D. Thesis, 1965.

7. Coon, J., Proc. Bergen Conference, 1965.

8. Eviatar, A., Univ. Maryland Tech. Note BN-429, Jan. 1966.

9. Fan, C. Y., G. Gloeckler, and J. A. Simpson, J.G.R. 71, 1837, 1966.

10. Fredricks, R. W., F. L. Scarf, and W. Bernstein, J.G.R. 70, 21, 1965.

11. Fredricks, R. W., and F. L. Scarf, J.G.R. 70, 4765, 1965.

12. Greenstadt, E. W., G. Inouye, I. Green, and D. Judge, Trans. AGU, 47, 143, 1966.

13. Harris, E. G., J. Nucl. Energy, Pt. C, 2, 138, 1961.

14. Hewish, A., P. F. Scott, and D. Wills, Nature 203, 1214, Sept. 19, 1964.

15. Holzer, R. E., M. G. McLeod, and E. J. Smith, J.G.R. 71, 1481, 1966.

16. Hundhausen, A. J., J. R. Asbridge, S. J. Bame, H. E. Gilbert, and I. B. Strong, Trans. A.G.U. 47, 147, 1966.

17. Kennel, C. F., and H. E. Petschek, J.G.R. 71, 1, 1966.

18. Meecham, W. C., J.G.R. 69, 3175, 1964.

19. Meyer, P., E. N. Parker, and J. A. Simpson, Phys. Rev. 104, 768, 1956.

20. Neugebauer, M., and C. W. Snyder, J.P.L. Preprint, 1966.

21. Noble, L. M., and F. L. Scarf, Astrophys. J. 138, 1169, 1963.

22. Noerdlinger, P. D., J.G.R. 69, 369, 1964.

23. Parker, E. N., Phys. Rev. 107, 923, 1957.

24. Parker, E. N., Astrophys. J. 128, 664, 1958.

25. Parker, E. N., Interplanetary Dynamical Processes (Wiley) 1963.

26. Parker, E. N., Space Science Rev. 4, 666, 1965.

27. Parker, E. N., Phys. Rev. Lett. 14, 55, 1965.

28. Rosenbluth, M. N., and R. F. Post, Phys. Fluids 8, 547, 1965.

29. Rostoker, N., Nucl. Fusion , 101, 1961.

30. Scarf, F. L., and L. M. Noble, A.I.A.A. J. 2, 1158, 1964.

31. Scarf, F. L., W. Bernstein, and R. W. Fredricks, J.G.R. 70, 9, 1965.

32. Scarf, F. L., and L. M. Noble, Astrophys. J. 141, 1479, 1965.

33. Scarf, F. L., J.G.R., June 1, 1966 (in press).

34. Scarf, F. L., J. H. Wolfe, and R. W. Silva, 1966, to be published.

35. Schaaf, S. A., and P. L., Chambrė, Flow of Rarified Gases (Princeton) 1961.

36. Snyder, C. W., and M. Neugebauer, Space Res., 4, 89, 1964.

37. Sonett, C. P., D. Judge, and J. Kelso, J.G.R. 64, 941, 1959.

38. Sonett, C. P., D. S. Colburn, L. Davis, Jr., E. J. Smith, and P. J. Coleman, Jr., Phys. Rev. Lett. 13, 153, 1964.

39. Spitzer, L., Jr., Physics of Fully Ionized Gases (Interscience) 1962.

40. Stix, T. H., The Theory of Plasma Waves (McGraw-Hill) 1962.

41. Stix, T. H., Phys. Fluids 7, 1960, 1964.

42. Strong, I. B., J. R. Asbridge, S. J. Bame, H. H. Heckman, and A. J. Hundhausen, Phys. Rev. Lett. 16, 631, 1966.

43. Sturrock, P. A., Phys. Rev. 141, 186, 1966.

44. Sturrock, P. A., and R. E. Hartle, Phys. Rev. Lett. 16, 628, 1966.

45. Tidman, D. A., Univ. of Maryland Tech. Note BN-426, Dec. 1965.

46. Van Allen, J. A., and S. M. Krimigis, J.G.R. 70, 5737, 1965.

47. Whang, Y. C., and C. C. Chang, J.G.R. 70, 4175, 1965.

48. Whang, Y. C., C. K. Lin, and C. C. Chang, Astrophys. J., in press.

49. Wolfe, J. H., R. W. Silva, and M. A. Meyers, COSPAR Rept., 1965.

50. Wolfe, J. H., R. W. Silva, D. D. McKibbin, and R. H. Mason, J.G.R., July 1, 1966 (in press).

APPENDIX B

A PLASMA INSTABILITY IN THE SOLAR WIND

by

F. L. Scarf

Space Sciences Laboratory
TRW Systems
Redondo Beach, California

and

J. H. Wolfe and R. W. Silva

Space Sciences Division
Ames Research Center
Moffett Field, California

ABSTRACT

Recent solar wind measurements on the Pioneer 6 spacecraft reveal that, in general, the proton velocity distribution is highly anisotropic with $T_{\parallel} >> T_{\perp}$, where the subscripts refer to direction with respect to the interplanetary magnetic field. A mechanism which can produce such an anisotropy is considered, and the consequences of this particle distribution with respect to stability of the plasma are analyzed. It is shown that a generalized form of the firehose instability must occur, with growth of magnetosonic (whistler mode) waves near the ion cyclotron frequency. Growth rates are computed for a range of wave frequencies and distances from the sun, and these predictions are compared with available interplanetary power spectra.